The Molecular Mechanisms of Ion-Specific Effects on Proteins

Kelvin B. Rembert[1], Jana Paterová[2], Jan Heyda[2], Christian Hilty[1], Pavel Jungwirth[2*], and Paul S. Cremer[1*]

[1]*Department of Chemistry Texas A&M University, 3255 College Station, TX 77843, USA*

[2]*Institute of Organic Chemistry and Biochemistry, Academy of Sciences of the Czech Republic, and Center for Biomolecules and Complex Molecular Systems, Flemingovo nám. 2, 16610, Prague 6, Czech Republic*

May 15, 2012

[*]Corresponding authors: pavel.jungwirth@uochb.cas.cz and cremer@chem.tamu.edu

Abstract: The specific binding sites of Hofmeister ions with an uncharged 600 residue elastin-like polypeptide, $(VPGVG)_{120}$, were elucidated using a combination of NMR and thermodynamic measurements along with molecular dynamic simulations. It was found that the large soft anions such as SCN^- and I^- interact with the polypeptide backbone via a hybrid binding site that consists of the amide nitrogen and the adjacent α-carbon. The hydrocarbon groups at these sites bear a slight positive charge, which enhances anion binding without disrupting specific hydrogen bonds to water molecules. The hydrophobic side chains do not contribute significantly to anion binding or the corresponding salting-in behavior of the biopolymer. Cl^- binds far more weakly to the amide nitrogen/α-carbon binding site, while SO_4^{2-} is repelled from both the backbone and hydrophobic side chains of the polypeptide. The Na^+ counterions are also repelled from the polypeptide. The identification of these molecular-level binding sites provides new insights into the mechanism of peptide-anion interactions.

Introduction

The influence of salts on biological function is ubiquitous, with specific choices of salt ions for particular tasks in living organisms being crucial.[1-3] For example, the cytosol is rich in potassium but poor in sodium, while the opposite is true for extracellular liquids.[4] Sodium exhibits slightly stronger affinity for proteins than potassium and could thus interfere at higher concentrations with the function of cellular enzymes.[5] Chloride, which interacts very weakly with proteins, is the universally present anion in biology.[4] By contrast, iodide, which is much rarer, as well as the toxic anions, perchlorate and thiocyanate, interact strongly with proteins particularly in the thyroid. The latter two anions are able to replace iodide and thus compromise thyroidal function.[6] Understanding the tight regulation and toxicity of various ions has been difficult due to the lack of identification of the molecular-level binding sites.

Previous studies have shown that the behavior of proteins and other polymers in aqueous salt solutions often follows a regular pattern that was first identified over 120 years ago.[1-7] This recurring trend in ion specificity is known as the Hofmeister series. Over the last half century, numerous efforts have been made to correlate the differences in the solubility of proteins in salt solutions to the various ion sizes, geometries, charge-to-volume ratios, entropies of hydration, and related physical properties.[8-13] The effects of the ions in the Hofmeister series are, however, typically only manifested above 10-100 mM salt concentration. This is relatively weak compared with numerous other biological interactions, which has made it hard to pinpoint the specific binding sites for ion-protein interactions.

To overcome this difficulty, we have undertaken a series of thermodynamic and proton NMR experiments in conjunction with molecular dynamic simulations on a model system consisting of the pentameric amino acid repeat, VPGVG. This biopolymer, known as an elastin-like polypeptide (ELP), is subject to an inverse phase transition as a function of temperature.[14] At low temperature, it is soluble in water, while above its lower critical solution temperature (LCST) the molecule undergoes hydrophobic collapse. The particular ELP employed in these experiments was V_5-120, where V_5 denotes the fact that all residues in the fourth position of the pentameric repeat were valines. Moreover, the macromolecule consisted of 120 pentameric repeats, so there were a total of 600 residues plus a very short leader and trailer sequence. ELP V_5-120 was investigated in a set of salt solution studies and displayed an LCST of 31 °C in the absence of salt. This phase transition temperature is known to be decreased by sodium salts in the following order:[15]

$$SO_4^{2-} > S_2O_3^{2-} > F^- > Cl^- > Br^- > NO_3^- > I^- > ClO_4^- > SCN^-$$

Anions to the left of chloride are strongly hydrated and lead to the hydrophobic collapse of the ELP, causing it to salt-out of solution.[8-11] On the other hand, anions to the right of chloride are weakly hydrated and help keep the biopolymer in solution in its uncollapsed state.

In the current study, we showed that increases in ELP solubility in the presence of large soft anions correspond to nonlinear changes in the relative proton chemical shifts at the α-proton and β-proton positions of the polypeptide as a result of anion binding. Decreases in ELP solubility when more strongly hydrated anions were introduced to solution corresponded to linear proton chemical shifts. The hydrophobic side chains of valine do not exhibit appreciable affinity to any of the investigated ions (Figure 1). These experimental results were complemented and confirmed by molecular dynamics simulations of the VPGVG peptide in the corresponding salt solutions. The present study also revealed a novel hybrid binding site composed of polar and nonpolar groups at the peptide backbone. Such findings should aide general predictions of the molecular level behavior of proteins in aqueous salt solutions.

Materials and Methods

ELP overexpression and purification

The details of ELP over expression and purification are reported elsewhere.[16,17] Briefly, ELP V_5-120 was over expressed in BLR/DE3 *E. Coli* in LB medium (Mo Bio TB dry High Nutrient Growth Media). Purification of ELP V_5-120 was accomplished by sonication of the cells to lyse them followed by two rounds of inverse transition cycling, whereby the ELP precipitated above its phase transition temperature. Samples were then dialyzed for two days against purified water with a minimum resistivity of 18 MΩ·cm using a Thermo Scientific Barnstead Nano pure water purification system. The concentration of V_5-120 was determined by measuring the absorbance at 280 nm, where $\varepsilon = 5690$ $M^{-1}cm^{-1}$.

LCST Measurements

The LCST was measured by turbidity on an automated melting point device with digital image processing software (MPA 100 Optimelt Automated Melting Point System – Stanford Research Systems). The intensity of light scattering was measured as a function of temperature using a ramp rate of 0.5 °C/min. The LCST values given herein corresponded to the onset of the increase in light scattering relative to the baseline.[18,19]

NMR measurements

NMR spectra for titrations of ELP with sodium salts were obtained on a 400 MHz NMR spectrometer equipped with a 5 mm TXI probe. ^{1}H spectra were acquired using W5 watergate or presaturation for water suppression.[20] All NMR samples were measured at 278 K, which is below the phase transition temperature of the ELP in all cases that were studied. Sample spectra were externally referenced to sodium 2,2-dimethyl-2-silapentane-5-sulfonate (DSS) (Cambridge Isotope Laboratories) in pure D_2O (D,99.9%, Cambridge Isotope Laboratories) in NMR tubes adapted with coaxial inserts (Wilmad-LabGlass). The DSS was always in the inner of the concentric tubes, while the ELP sample was in the outer tube. As such, the DSS control was never exposed to the ELP or varying salt concentrations. Spectra for the chemical shift assignments of the biopolymer were acquired on the 400 MHz spectrometer and on a 500 MHz spectrometer with a CryoProbe TCI (Bruker, Billerica, MA, USA). Spectra were obtained in [^{1}H,^{1}H]-NOSEY (100 ms mixing time), double quantum filtered [^{1}H,^{1}H]-COSY and [^{1}H,^{1}H]-TOCSY (100 ms mixing time) experiments,[21] as well as with [^{1}H,^{13}C]-HSQC and multiple [^{1}H,^{13}C]-HMBC (J-filter ranges between 4 and 20 Hz).[22] TopSpin software (Bruker) and Mnova software (Santiago de Compostela, Spain) were used for data processing.

Sample Preparation

The NaSCN, NaI, and Na_2SO_4 employed in these experiments were purchased from Sigma Aldrich (St. Louis, MO), while NaCl came from VWR (Radnor, PA). All salts were at least 98% pure and employing even higher purity salts did not change the NMR spectra or the LCST data. Polyacrylamide was purchased from Aldrich. Poly(*N,N*-dimethylacrylamide) was synthesized by the group of David E. Bergbreiter at Texas A&M. Salt and polymer solutions were prepared with 18 MΩ·cm purified water. Stock solutions of salts and ELPs were prepared at double the desired concentration and mixed 1 to 1 (volume to volume) to obtain the desired sample concentration. The total ELP V_5-120 polymer concentration in all experiments was 3.5 mg/mL (70 μM). This corresponds to an amino acid monomer concentration of ~42 mM. Control experiments with poly(*N,N*-dimethylacrylamide) and poly(acrylamide) were also performed at concentrations such that the corresponding monomer equivalents were also ~42 mM.

Molecular Dynamics Simulations

For computational studies, the VPGVG pentapeptide (described using the polarizable version of the parm99SB force field[23]) was solvated in 1 M NaCl,[24,25] 1 M NaSCN,[26] or in 0.333 M Na_2SO_4[27] (i.e., employing the same ionic strength for all solutions). The system thus consisted of a single pentapetide, 2400 water molecules (POL3),[28] 45 cations, and 45 anions (or 30 cations and 15 anions for sulfate), which led to an equilibrium box size of approximately $42.7 \times 42.7 \times 42.7$ Å. Note that the polarizabilities employed are typically smaller than the experimental estimates, in order to avoid the so called "polarization catastrophe"[29] and to avoid over polarizing the system.[30]

The system was constrained at ambient conditions (300 K and 1 atm) via coupling to the Berendsen thermostat and barostat.[31] 3D periodic boundary conditions were applied with long-range electrostatic interactions beyond the non-bonded cutoff of 8 Å accounted for using the particle mesh Ewald (PME) method.[32] Polarization effects were included within a self-consistent iterative procedure. All bonds containing hydrogens were constrained using the SHAKE algorithm.[33]

The total simulation time for each run was 100 ns (after equilibration for 1 ns) with a time step of 1 fs. The coordinates were saved every 1 ps yielding 100 000 frames for further analysis. The simulation length was sufficient to provide converged data on ion interactions with the peptide surface. All molecular dynamics calculations were performed using the AMBER11 program.[34]

Two different sets of calculations were performed. In the first case, the peptide was constrained to an extended conformation, mimicking the extended structure of a building block of the experimental elastin-like polymer. In the second case, the peptide was completely free to move and therefore able to sample a large variety of conformations. It should be noted that we only aimed at simulating the ionic distributions around the peptide in the uncollapsed state rather than the hydrophobic collapse process of the entire macromolecule. Simulating hydrophobic collapse would not only have required a much longer peptide, but also prohibitively long simulation times.

Results

$ELPV_5$-120 solubility as a function of salt concentration

Figure 2 plots the change in the LCST (ΔT) of the ELP as a function of salt concentration for three cases: NaSCN, NaCl, and Na$_2$SO$_4$. As can be seen, the LCST decreases linearly as NaCl and Na$_2$SO$_4$ are added to solution. By contrast, NaSCN leads to an increase in the LCST in a nonlinear fashion. The data for NaSCN can be fit by eqn. 1, which consists of a linear term plus a binding isotherm:[15]

$$\Delta T = -c[M] + \frac{B_{max}[M]}{K_D + [M]} \qquad \text{eqn. 1}$$

In the first term, the constant, c, which has units of temperature divided by molar concentration, is the line slope and [M] is the salt concentration. The second term, the binding isotherm, contains the apparent equilibrium dissociation constant, K_D, as well as the constant B_{max}, which represents the maximum increase in the LCST caused by the binding of ions. As such, B_{max} has units of temperature, while K_D is in units of concentration. The data for NaCl and Na$_2$SO$_4$ can also be fit to eqn. 1 by assuming an infinitely weak binding interaction. In thermodynamic models, salting-in has been associated with ion accumulation at the macromolecule/water interface, while salting-out has been associated with ion depletion.[35]

ELPV$_5$-120 binding sites probed by NMR

To probe the molecular-level mechanism for changes in the phase transition temperature with salt, proton NMR experiments were conducted with the same three salts at a constant temperature of 5 °C, which is below the LCST of the ELP under all conditions. Figure 3 shows the assignments of the protons in ELP V$_5$-120 in salt free aqueous solution. Different protons in the spectrum displayed markedly different behavior as salt was added to solution. The change in the chemical shift for the α-protons of the glycine residues are plotted in Figure 4a. As can be seen, these protons shifted in a fashion that was reminiscent of the thermodynamic data. Specifically, in the presence of NaSCN, the change in the chemical shift displayed markedly nonlinear behavior. Such a result is consistent with the notion that SCN$^-$ and to a much lesser extent Cl$^-$ interact with the methylene units in the polypeptide backbone. The curves for the chemical shift were fit to eqn. 2:

$$\Delta\delta = -c[M] + \frac{\Delta\delta_{max}[M]}{K_D + [M]} \qquad \text{eqn. 2}$$

This equation has the identical form as eqn. 1, where the left-hand-side is now the change in chemical shift, $\Delta\delta$, with respect to salt-free sample. In this case, the linear constant, c, has units of chemical shift

divided by molar concentration, whereas $\Delta\delta_{max}$ is the maximum change in the chemical shift for the nonlinear portion of the curve at saturation.

By contrast to the data in Figure 4a, the methyl protons from the valine residues displayed only linear changes in their chemical shift for all three sodium salts (Figure 4b). The proton shift for water[36] also varied in a linear fashion (Figure 4c). The linear shift in the water protons as well as those on hydrophobic side chains is consistent with the linear salting-out effect from the thermodynamic data in Figure 2. Moreover, the linear salting-out of the ELP can be correlated with increasing surface tension at the polymer/water interface when the sodium salts of weakly hydrated anions are added to solution.[15] For strongly hydrated anions, the salting-out behavior has been shown to correlate with the entropy of hydration of the anions. This is essentially an excluded volume effect, since well hydrated anions remain in the bulk solution and are therefore depleted from the polypeptide/water interface.

An additional potential site for interactions of weak hydrated anions involves the NH protons of the amide groups. The addition of NaSCN leads to a decidedly nonlinear change in the chemical shift of the NH protons (Figure 5a). This is expected as the NH protons and α-protons are in close proximity. By contrast, NaCl led to much less curvature in the concentration dependence of the chemical shift, while virtually none was observed for SO_4^{2-}. Since the data in Figure 4a appear to indicate that there are interactions between SCN^- and the amide NH groups, it is important to probe these putative interactions in the absence of an adjacent aliphatic group that can act as a binding site. To do this, control experiments were performed with polyacrylamide in water using NaSCN. As can be seen, the nonlinearity of the chemical shift becomes much less pronounced (Figure 4b). Upon methylation of poly(acrylamide) to poly(*N,N*-dimethylacrylamide), however, the chemical shift of the methyl protons again show pronounced binding behavior (Figure 4c). Such a result is consistent with previous thermodynamic studies, which indicated that the apparent binding constants for weakly hydrated anions are at least two orders of magnitude tighter when at least one of the NH groups of the acrylamide side chain is methylated.[37-38]

Although, the data described above indicate that the binding site for weakly hydrated anions involves the α-position of the polypeptide, there are probably varying degrees of interactions with multiple backbone sites. Chemical shift data were collected for all CH_n protons on the ELP. In addition to deviations from linearity for protons associated with the α-carbons, less pronounced curvature also could be seen from β-protons and the proline ring. These effects can be displayed by subtracting the linear portion of the chemical shift changes and plotting the residuals (Figure 6). All such data fit well to a simple binding isotherm. The apparent K_D values for the varying sites ranged from ~50 mM for the protons on the α-carbons of glycine and the methylene adjacent to nitrogen on the proline ring to ~270

mM for the β-carbons and other proline ring methylene groups. The dissociation constant approached infinity for the protons from the methyl groups of the valine residues. The apparent equilibrium dissociation constants from Langmuir isotherm fitting are provided in Table 1. One can also abstract the nonlinear portion of the LCST data for the ELP in the presence of varying concentrations of NaSCN. This residual data is also plotted in Figure 6 (blue squares along with an arrow to the right) and the y-axis in this case involves ΔLCST instead of Δδ. The apparent K_D value from the LCST data is 390 mM, which should correspond to an averaged value over the varying sites on the polypeptide. It is slightly weaker than the values abstracted from NMR because thermodynamic measurements were made at the LCST of the ELP, which was always higher than the 5 °C used in the spectroscopic measurements. It should be noted that the identical NMR and LCST measurements for these three salts were repeated with NaI (Figures S11- S16). The results were nearly identical with those of NaSCN, although the I⁻ interacted more weakly with the amide NH.

VPGVG pentapeptide - ion binding probed by MD simulations

Using MD simulations with polarizable potentials we analyzed the distributions of the three anions – SCN⁻, Cl⁻, and SO_4^{2-} and the Na⁺ cation around an aqueous VPGVG pentapeptide. The terminal charges of the pentapeptide were removed by acetylating the *N*-terminus and methylating the *C*-terminus. Since the ELP is extended and unfolded below the LCST,[39] we have also constrained the pentapeptide to an extended geometry to better mimic the experimental situation. Ion distributions around an unconstrained pentapeptide, which explores both extended and more compact geometries are, nevertheless, very similar (see Figs. S9 and S10 in Supporting Information). Figure 7 shows the distributions of ions around VPGVG averaged over 100 ns simulations in 1 M NaSCN and NaCl, and 0.33 M Na_2SO_4. The plots correspond to an isovalue of 5 times the bulk ion concentration. One immediately sees that there are extended regions around the pentapeptide where SCN⁻ is significantly enhanced. By contrast, the spatial regions of enhanced concentrations are restricted to very narrow regions opposing the peptide N-H groups for Cl⁻ and SO_4^{2-}, and the C=O groups for Na⁺. Also, despite the fact that the SCN⁻ and Cl⁻ distributions are very different, the Na⁺ distributions in the two solutions are very similar to each other, which points to very weak cation-anion interactions in these systems. Even for Na_2SO_4, where non-negligible pairing between Na⁺ and SO_4^{2-} occurs, the sodium distribution does not differ much from the previous two cases.

The interaction 'hotspots' for the pentapeptide can be quantitatively analyzed by cutting the space around VPGVG into regions closest to the peptide bond or the CH_n groups. The latter were further

divided into two groups giving either non-linear or linear concentration dependent NMR signals. The terminal capping groups were excluded from this analysis. The proximal distribution functions of SCN^-, Cl^-, SO_4^{2-}, and Na^+ around VPGVG for these three regions are presented in Figure 8. We see that SCN^- interacts with the three regions of VPGVG in a non-uniform fashion. The interactions with the N-H side of the peptide bonds and the adjacent αCH_n groups are the strongest, while interactions with the NMR linear valine methyl groups are weaker. The interactions with the former two groups are cooperative and cannot be strictly separated, as demonstrated by extended regions of enhanced SCN^-concentration around the peptide backbone (Figure 7). For Cl^- and SO_4^{2-}, all these interactions are significantly reduced compared to SCN^-, with the latter being repelled from all CH_n groups. Finally, Na^+ exhibits affinity solely to the C=O sides of the peptide bonds, being repelled from all CH_n groups. Note that the effects of polarization on the interactions of these ions with VPGVG are very small except for the case of SCN^-, where polarization increases the binding to some extent (see Supporting information for comparison to a non-polarizable simulation).

Probably the best way to analyze the MD results in the light of the above experimental observations is in terms of the preferential bindings of ions with respect to water[40] in these three spatial regions around the peptide. The preferential binding curves plotted are integral quantities which converge to a finite value at large distances. If this value is positive (or negative), there is net attraction (or net repulsion) of ions from the peptide. The insets in Figure 8 depict such plots (i.e., excesses of the SCN^-, Cl^-, SO_4^{2}, and Na^+ ions over water, normalized to zero for the bulk solution) separately for the three spatial regions around VPGVG. It is immediately clear that SCN^- exhibits strong preferential binding to the peptide bonds and the immediately adjacent CH_n groups. There is also a weak and radially limited region of enhanced SCN^- concentration around the valine methyl groups; however, this is overcompensated by regions of decreased SCN^- concentrations further away and, as such, there is no preferential binding. The net preferential binding of Cl^- and SO_4^{2-} to the peptide bonds and the adjacent NMR non-linear CH_n groups is slightly negative, while that to methyl groups of valine is strongly negative. Sodium exhibits some preferential binding at the peptide bonds; however, its net effect is rather weak due to the very narrow cone of enhancement of Na^+ opposite to C=O groups. Moreover, Na^+ has a significantly negative preferential binding to all CH_n groups, leading to net exclusion from the uncharged polypeptide.

Discussion

The NMR and MD simulation data clearly demonstrate that the salting-in behavior of NaSCN is primarily caused by the binding of the weakly hydrated SCN^- anion with the polypeptide backbone of the

ELP. The enhanced interaction of SCN$^-$ with CH$_n$ groups next to heteroatoms like nitrogen (or oxygen) is connected with the electron-withdrawing ability of these atoms from the neighboring groups. Due to this effect, the overall charge on the CH$_n$ groups corresponding to α-carbon atoms and the proline heteroring is slightly positive (around +0.1 e), while that of the CH$_3$ groups on valine side chains is weakly negative (-0.08e), as reflected in the force field of the present simulations[41] (Supporting Information, Figure S6). The formal positive charge naturally enhances the binding of large soft anions, such as SCN$^-$. A similar effect is also observed for iodide (see Figures S11 and S18 in Supporting Information). In addition, hydrogen bonding to the neighboring NH groups helps the interaction of SCN$^-$ with the adjacent CH$_n$ group, but it is not essential. This is demonstrated by a simulation, where all the backbone NH groups were methylated (Supporting Information, Figures S7 & S8). Such methylation prevents the formation of backbone-SCN$^-$ hydrogen bonds. Nevertheless, the total amount of SCN$^-$ binding to the peptide is only weakly affected. As such, the binding site for peptide amide groups is an inseparable combination of polar and non-polar units.

The hybrid hydrophobic/hydrophilic binding site does not require specific hydrogen bonds between water and the polypeptide to be broken, since water only hydrophobically hydrates the methylene units without strong OH directionality in the absence of salt. By contrast, binding between anions and the amide NH moiety requires breaking of water-peptide hydrogen bonds and would therefore be less favorable on enthalpic grounds. The idea that weakly hydrated anions will not bind significantly with generic alkyl chains is in good agreement with previous thermodynamic studies that showed that hydrophobic moieties lead to salting-out of molecules even in the presence of the most weakly hydrated anions.[15] Indeed, weakly hydrated anions do not bind appreciably with methyl groups that are not either directly bonded to an electron withdrawing atom or next nearest neighbors with an electron withdrawing atom. Such a result is somewhat analogous to the findings for weakly hydrated anions at the aqueous/vapor interface, although the polymer/water interface is considerably more complex.[42-43]

The amide backbone binding sites for weakly hydrated anions are the most significant locations for the salting-in of uncharged polypeptides. Such binding will lead to a saturation binding isotherm. However, even the most weakly hydrated anions also can cause salting-out behavior by increasing the surface tension of the purely hydrophobic portions of the polymer/water interface.[9,15,38] In other words, specific binding sites lead to net anion inclusion, but once those sites are saturated, further increases in salt concentration actually lead to net anion exclusion. Therefore, weakly hydrated anions display duel salting-in and salting-out behavior. By contrast, the interactions of strongly hydrated anions with uncharged and non-polar residues on the peptide chain only lead to salting-out effects. Their exclusion from the polypeptide/water interface leads to hydrophobic collapse and aggregation on entropic grounds

(i.e. an excluded volume effect). This is similar to the behavior of most cations such as Na^+, which are also strongly excluded from the polypeptide backbone. The general exclusion of most cations from the polymer/water interface is the reason why specific cation effects are far less pronounced than anion effects, which show far richer chemistry. Both strongly hydrated anions (e.g. SO_4^{2-}) and cations (e.g. Na^+) can, of course, bind significantly with charged protein side chains and this may lead to salting-in behavior when the appropriate residues are present.

The solubility and self-assembly behavior of organic molecules in aqueous solutions has been traditionally assumed to depend upon the separate contributions of charged, polar, and hydrophobic groups. This also applies to amino acid side chains; however, we have demonstrated above that ion binding to polypeptide backbones is dominated by the unique nature of the non-polar/polar α-carbon binding sites. Such interactions along with ion pairing[3,5,44] in the presence of charged residues, dominate the Hofmeister chemistry of proteins. Beyond Hofmeister effects, the phase behavior of macromolecules and amphiphiles can be tuned by taking advantage of the unique properties of hybrid polar/non-polar sites. Nature almost certainly does this. For example, one of the strongest protein stabilizers *in vivo* is trimethylamine *N*-oxide (TMAO), which contains three modestly hydrophilic methyl groups directly bound to the nitrogen atom of an NO moiety.[45] These methyl groups actually orient away from hydrophobic interfaces,[46] which may help explain this osmolyte's ability to stabilize folded protein structure. A synthetic example of a hybrid polar/non-polar site comes from the cyclic cavities of triazophanes, which can capture anions.[47] Knowledge of how to synthesize and exploit hybrid polar/non-polar sites may allow the creation of new materials, sensor devices, and novel self-assembled structures.

Associated content

Supporting Information

LCST, NMR, and MD results for NaI, the effect of pH on the LCST of the ELP and the amide proton chemical shift, chemical shift titrations demonstrated by multiple spectra display, distribution of partial charges on VPGVG, and ion distributions around VPGVG with methylated N-H bonds and around unconstrained VPGVG. This material is available free of charge via the Internet at http://pubs.acs.org.

References

1. Kunz, W., Lo Nostro, P., Ninham, B.W., *Curr. Opin. Colloid Interface Sci.*, **9**, 1-18, (2004)

2. Tobias, D.J., Hemminger, J.C., *Science*, **319**, 1197-1198, (2009)

3. Collins, K.D., *Biophys. Chem.*, **119**, 271-281, (2006)

4. Darnell, J., Lodish, H., Baltimore, D., Molecular Cell Biology (Scientific American Books, New York), (1990).

5. Vrbka, L.,Vondrasek, J., Jagoda-Cwiklik, B., Vacha, R., Jungwirth, P., *Proc. Natl. Acad. Sci. U. S. A.*, **103**, 15440-15444, (2006)

6.Braverman, L. E., He, X., Pino, S., Cross, M., Magnani, B., Lamm, S. H.,Kruse, M. B., Engel, A., Crump, K. S., Gibbs, J. P., J. Clin. Endocrinol.Metab. **90**, 700-706 (2005)

7. Hofmeister, F., Arch. Exp. Pharmakol. **24**, 247-260 (1888)

8. Robinson, D.R., Jencks, W.P., *J. Am. Chem. Soc.*, **87**, 2470-2479 (1965)

9. Baldwin, R.L., *Biophys. J.*, **71**, 2056-2063 (1996)

10. Zhang, Y.J., Cremer, P.S., *Curr. Opin. Chem. Bio.*, **10**, 658-663 (2006)

11. Collins, K.D., *Proc. Natl. Acad. Sci.*, **92**, 5553-5557 (1995)

12. Omta, A.W., Kopman, M.F., Woutersen, S., Bakker, H.J., *Science*, **301**, 347-349 (2003)

13. Kalcher, I., Horinek, D., Netz, R.R., Dzubiella, J., *J. Phys. Condens. Matter*, **21**, 424108 (2009)

14. Meyer, D.E., Chilkoti, A., *Nature Biotechnology*, **17**, 1112-1115 (1999)

15. Cho, Y.H., Zhang, Y.J., Christensen, T., Sagle, L.B. Chilkoti, A., Cremer, P.S., *J. Phys. Chem. B.*, 112, 13765-13771 (2008)

16. K. Trabbic-Carlson, L. Lui, B. Kim, A. Chilkoti, *Protein Science* **13,** 3274 (2004).

17. D. E. Meyer, A. Chilkoti, *Biomacromolecules* **3,** *357* (2002).

18. B. A. Deyerle, Y. Zhang, *Langmuir,* **27**, 9203 (2011).

19. H. G. Schild, D. A. Tirrell, *J. Phys. Chem.***94**, 4352 (1990).

20. M. Liu et al., J. Magn. Reson.**132**, 125-129 (1998).

21. K. Wüthrich, <u>*NMR of Proteins and Nucleic Acids*</u>, Wiley-Interscience, (1986).

22. C.E. Hadden et al., J. Magn. Reson.**140**, 274-280 (1999).

23. J. M. Wang, R. M. Wolf, J. W. Caldwell, P. A. Kollman, D. A. Case, *J. Comput. Chem., 25,* 1157 (2004).

24. L. Perera, M. L. Berkowitz, *Journal of Chemical Physics***95**, 1954 (1991).

25. L. Perera, M. L. Berkowitz, *Journal of Chemical Physics* **100,** 3085 (1994).

26. P. B. Petersen, R. J. Saykally, M. Mucha, P. Jungwirth, *J. Phys. Chem. B, 109*, 13402 (2005).

27. E. Wernersson, P. Jungwirth, *J. Theor. Comput. Chem.*, ***6,*** 3233- (2010).

28. J. W. Caldwell, P.A. Kollman, *J. Phys. Chem.* **99,** 6208 (1995).

29. Thole, B.T., *Chem. Phys.*, ***59***, 341-350 (1981)

30. Wick, C.D., *J. Chem. Phys.*, ***131***, 084715 (2009)

31. H. J. C. Berendsen, J. P. M. Postma, W. F. Vangunsteren, A. Dinola, J. R. Haak, *J. Chem. Phys., 81,* 3684 (1984).

32. U. Essmann, L. Perera, M. L. Berkowitz, T. Darden, H. Lee, L. G. Pedersen, *J. Chem. Phys., 103,* 8577 (1995).

33. J. P. Ryckaert, G. Ciccotti, H. J. C. Berendsen, *J. Comput. Phys., 23,* 327 (1977).

34. D.A. Case, T. A. D., T.E. Cheatham, III, C.L. Simmerling, J. Wang, R.E. Duke, R. Luo, R.C. Walker, W. Zhang, K.M. Merz, B. Roberts, B. Wang, S. Hayik, A. Roitberg, G. Seabra, I. Kolossvai, K.F. Wong, F. Paesani, J. Vanicek, J. Liu, X. Wu, S.R. Brozell, T. Steinbrecher, H. Gohlke, Q. Cai, X. Ye, J. Wang, M.-J. Hsieh, G. Cui, D.R. Roe, D.H. Mathews, M.G. Seetin, C. Sagui, V. Babin, T. Luchko, S. Gusarov, A. Kovalenko, and P.A. Kollman; Amber **11,** University of California, San Francisco: San Francisco, (2010).

35. Pegram, L.M., Record, M.T., *J. Phys. Chem B*, **31**, 9428-9436 (2008)

36. Maemets, V., Koppel, I, *J. Chem. Soc., Faraday Trans.*, **94**, 3261-3269 (1998)

37. VonHippel, P.H., Peticola, V., Schlack, L., Karlson, L., *Biochemistry*, **12**, 1256-1264 (1973)

38. Zhang, Y.J., Furyk S., Bergbreiter, D.E., Cremer, P.S., *J. Am. Chem. Soc.*, **127**, 14505-14510 (2005)

39. Cho, Y.H., Sagle, L.B., Iimura, S., Zhang, Y.J., Kherb, J., Chilkoti, A., Scholtz, J.M., Cremer, P.S., *J. Am. Chem. Soc.*, **131**, 15188-15193 (2009)

40. Li, W., My, Y., *J. Phys. Chem.* **135**, 134502 (2011)

41. Hornak, V., Abel, R., Okur, A., Strockbine, B., Roitberg, A., Simmerling, C., *Proteins* **65**, 712–725 (2006).

42. Jungwirth, P., Tobias, D.J., *Chem. Rev.*, **106** (1259-1281 (2006)

43. Arslanargin, A., Beck, T.L., *J. Chem. Phys.*, **136,** 104503 (2012)

44. Marcus, Y, Glenn, H., Chem. Rev., **106**, 4585-4621 (2006)

45. Koga, Y., Westh, P., Nishikawa, K., Subramanian, S., *J. Phys. Chem. B*, **115**, 2995-3002 (2011)

46. Sagle, L.B., Cimatu, K., Litosh, V.A., Liu, Y., Flores, S.C., Chen, X., Yu, B., Cremer, P.S., *J. Am. Chem. Soc*., **133**, 18707-18712 (2011)

47. Li, Y.J, Flood, A.H., *Angew. Chem. Int. Ed*., **47**, 2649-2652 (2008).
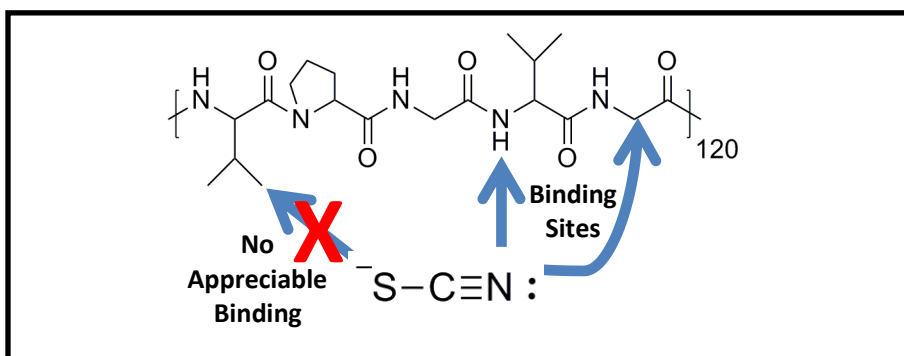
Figure 1. Schematic diagram depicting the molecular level binding sites for SCN⁻ with (VPGVG)ₙ. As shown, the anion binds preferentially to the methylene moiety within the amide backbone, but not appreciably to a purely hydrophobic methyl group such as the ones on valine. The anion also binds to some extent with the NH proton. It should be noted that only one resonance structure of SCN⁻ is depicted. The other one consists of two double bonds and the placement of the formal charge on the nitrogen atom.
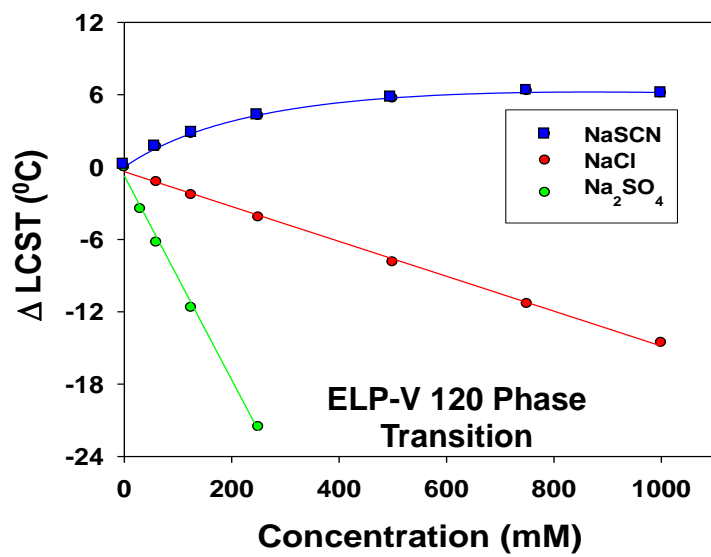
Figure 2. LCST of ELP-V$_5$-120 as a function of salt concentration for NaSCN, NaCl, and NaSCN.
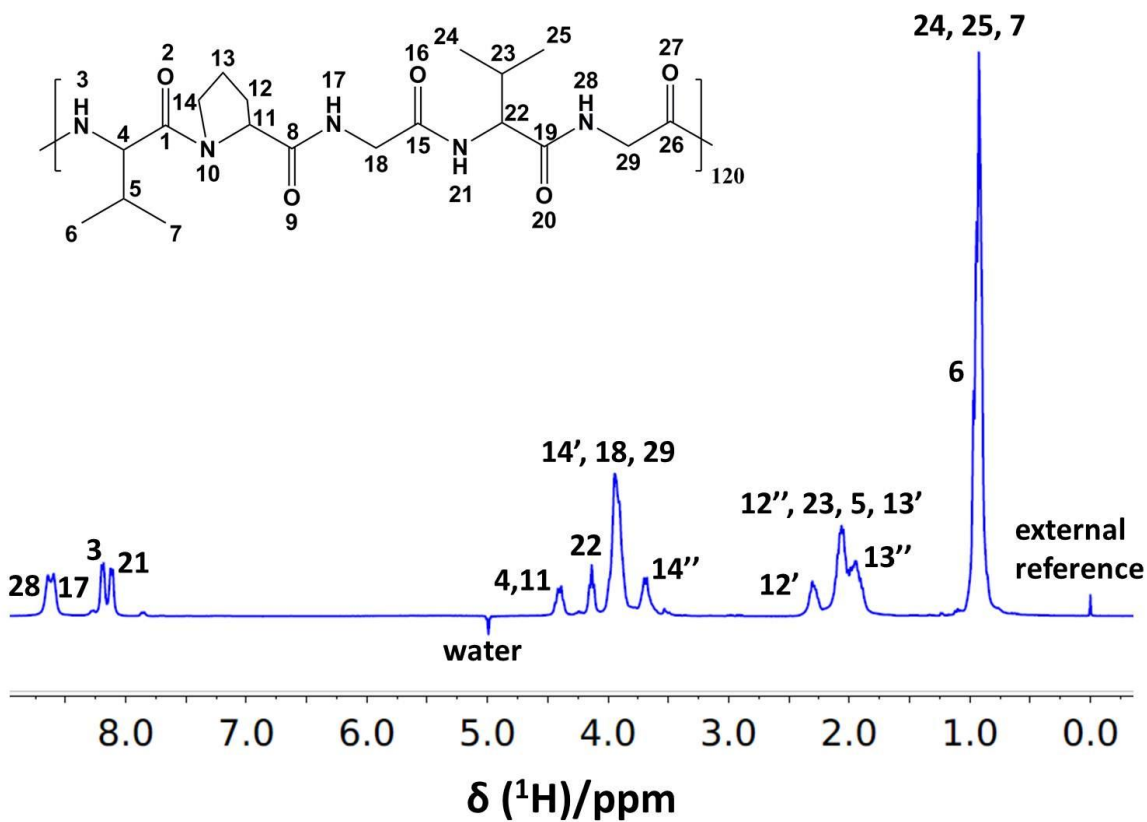
Figure 3. Proton NMR spectrum showing assignments of ELP- V_5-120 at 278K in a salt-free aqueous solution. The spectrum was externally referenced to DSS. The numbering at the proton resonances corresponds to atomic positions in the VPGVG pentapeptide above.
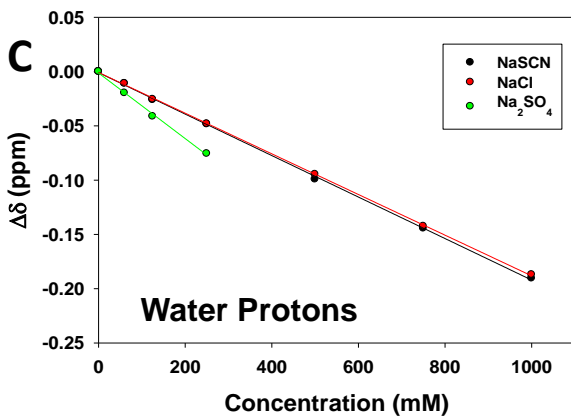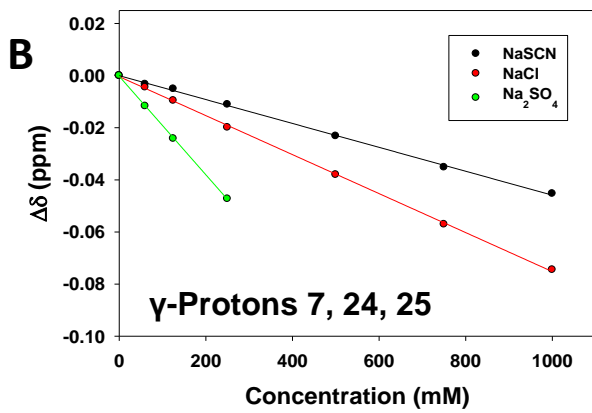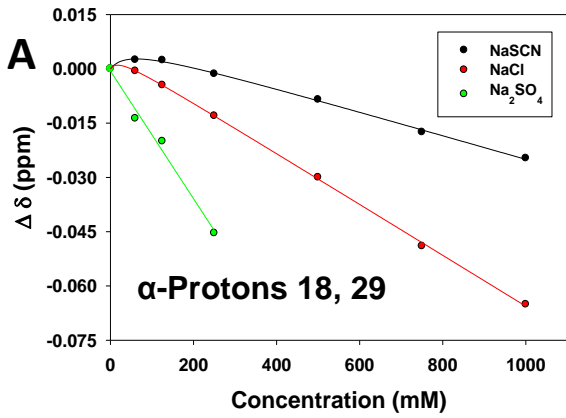
Figure 4. The chemical shift change as a function of concentration of three salts for (A) the α-protons of glycine, (B) the methyl protons of valine, and (C) the water protons.
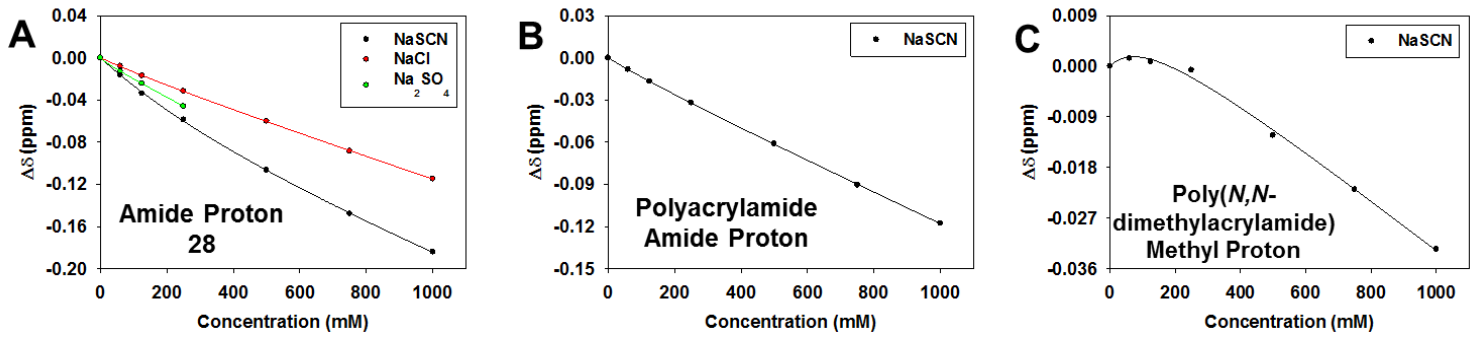
Figure 5. The chemical shift change for (A) the amide protons of ELP-V$_5$-120, (B) the amide protons of poly(acrylamide), and (C) the methyl protons of poly(*N,N*-dimethylacrylamide).
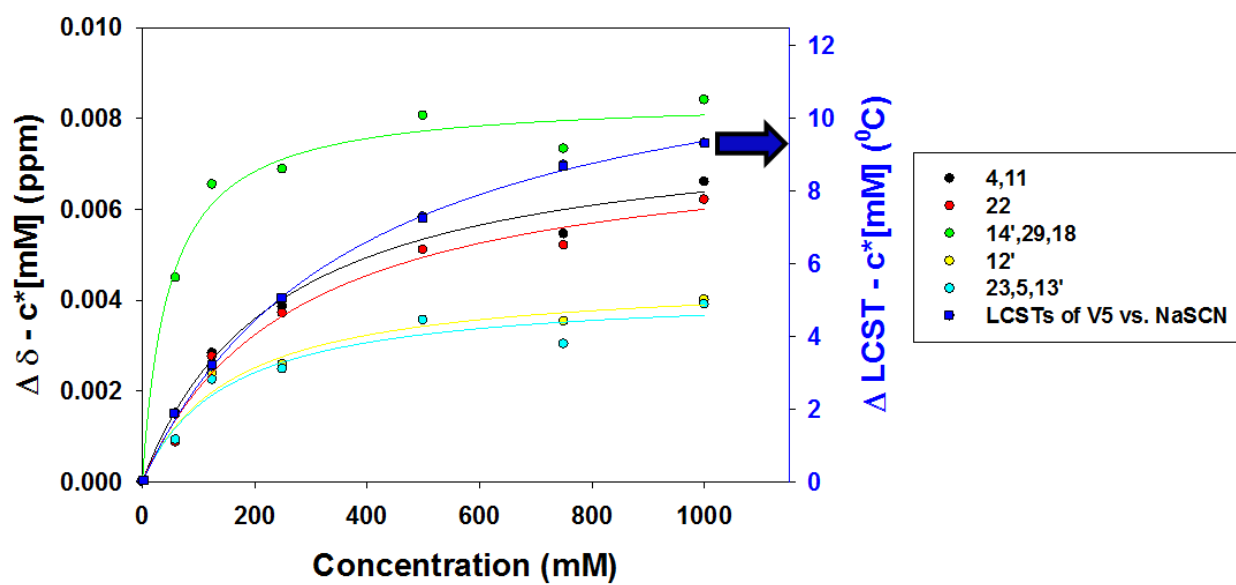
Figure 6. The residual change after subtraction of linear portion in the chemical shift for the protons from ELP-V$_5$-120 in the presence of NaSCN plotted together with the residual change in the LCST.
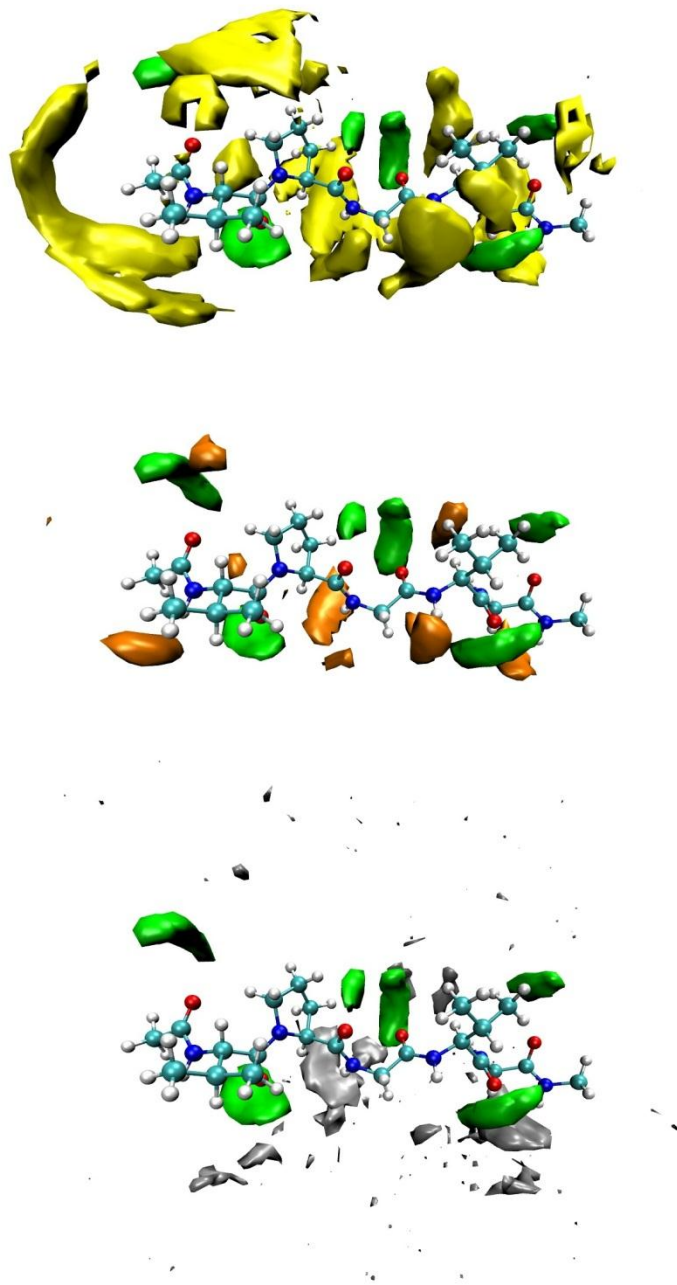
Figure 7. Distributions of SCN$^-$(yellow), Cl$^-$ (orange), SO$_4^{2-}$ (grey), and Na$^+$ (green) around the extended VPGVG peptide, as obtained by averaging over 100 ns molecular dynamics simulations in 1 M sodium salt solutions (or 0.33 M for Na$_2$SO$_4$, yielding the same ionic strength as for the 1 M monovalent salts).
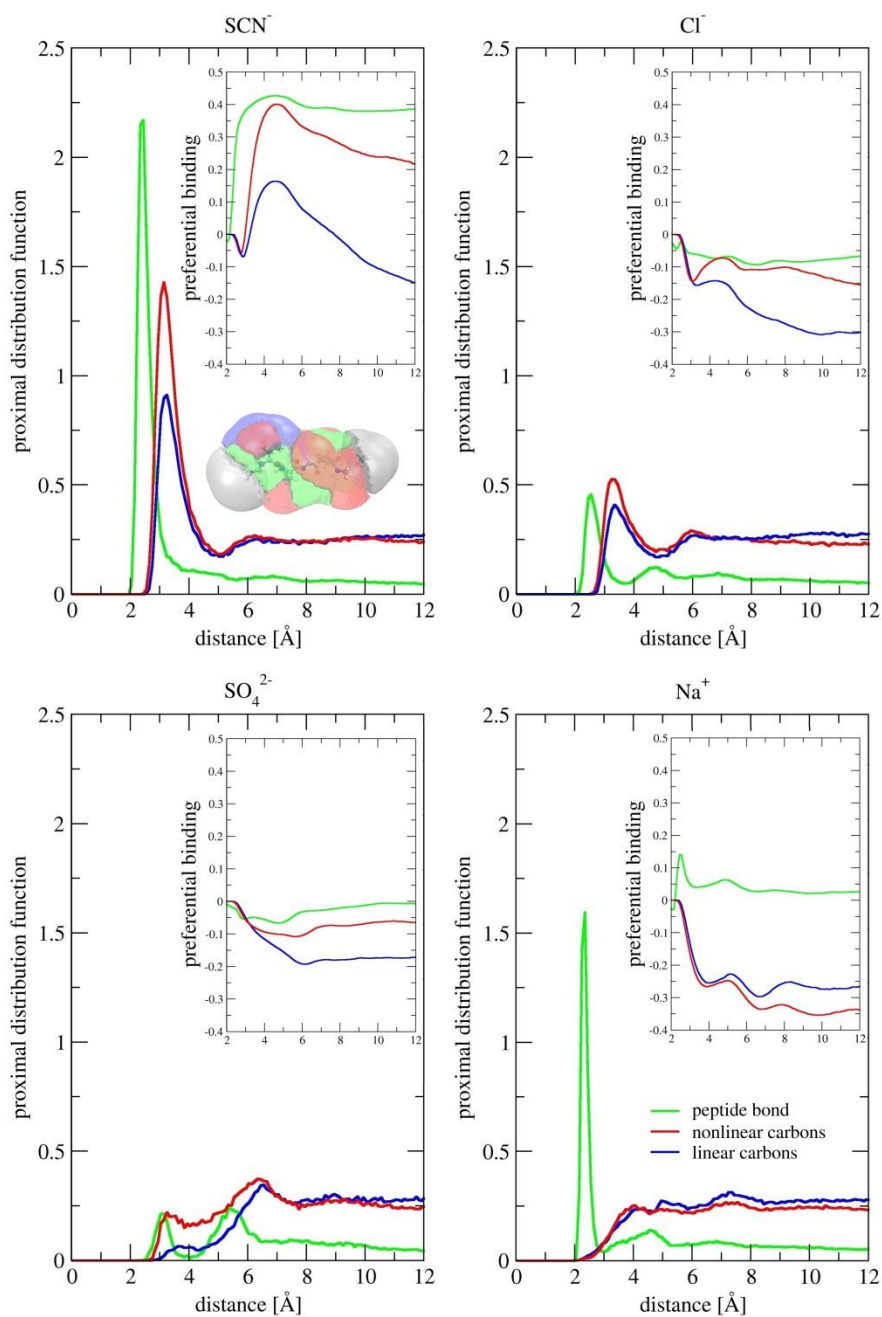
Figure 8. Proximal distribution functions of SCN^-, Cl^-, SO_4^{2-}, and Na^+ to groups forming the peptide bond (green), the adjacent CH_n groups giving rise to a non-linear salt concentration dependence of the NMR signal (red), and the CH_n groups giving rise to a linear NMR signal (blue). The corresponding three spatial regions around the peptide are shown schematically using the same colors as depicted in the upper left figure (the capping groups are depicted in grey). Insets: Preferential bindings of the four ions with respect to water to the above three groups of the VPGVG peptide (color coding is the same as in the main figures).

Table 1. Apparent equilibrium dissociation constants abstracted from isotherm fitting of the LCST and NMR data of ELP V_5-120 in the presence of NaSCN.

Proton Position	Kd (mM)
4,11	240
22	270
14' , 29 , 18	50
12'	160
23 , 5 , 13'	150
LCST of ELP-V$_5$ 120	390

TOC Figure